

VISION-R1: INCENTIVIZING REASONING CAPABILITY IN MULTIMODAL LARGE LANGUAGE MODELS

Wenxuan Huang^{1,2*}† Bohan Jia^{1*} Zijie Zhai¹ Shaosheng Cao³✉

Zheyu Ye³ Fei Zhao³ Zhe Xu³ Yao Hu³ Shaohui Lin^{1✉}

¹East China Normal University ²The Chinese University of Hong Kong ³Xiaohongshu Inc.

wxhuang0616@gmail.com (Wenxuan Huang)

*: Equal Contribution †: Project Leader ✉: Corresponding Author

ABSTRACT

DeepSeek-R1-Zero has successfully demonstrated the emergence of reasoning capabilities in LLMs purely through Reinforcement Learning (RL). Inspired by this breakthrough, we explore how RL can be utilized to enhance the reasoning capability of MLLMs. However, direct training with RL struggles to activate complex reasoning capabilities such as questioning and reflection in MLLMs, due to the absence of substantial high-quality multimodal reasoning data. To address this issue, we propose the reasoning MLLM, *Vision-R1*, to improve multimodal reasoning capability. Specifically, we first construct a high-quality multimodal CoT dataset without human annotations by leveraging an existing MLLM and DeepSeek-R1 through modality bridging and data filtering to obtain a 200K multimodal CoT dataset, *Vision-R1-cold dataset*. It serves as cold-start initialization data for Vision-R1. To mitigate the optimization challenges caused by overthinking after cold start, we propose *Progressive Thinking Suppression Training (PTST)* strategy and employ Group Relative Policy Optimization (GRPO) with the hard formatting result reward function to gradually refine the model’s ability to learn correct and complex reasoning processes on the multimodal math dataset. Comprehensive experiments show our model achieves an average improvement of $\sim 6\%$ across various multimodal math reasoning benchmarks using only a 10K multimodal math data during RL training. Vision-R1-7B achieves a 73.5% accuracy on the widely used MathVista benchmark, which is only 0.4% lower than the leading reasoning model, OpenAI O1. Scaling up the amount of multimodal math data in the RL training, Vision-R1-32B and Vision-R1-72B achieves 76.4% and 78.2% MathVista benchmark scores, respectively. The datasets, weight and code will be released in: <https://github.com/Osilly/Vision-R1>.

1 INTRODUCTION

Enhancing the complex reasoning capability of Large Language Models (LLMs) remains one of the most challenging problems in Artificial Intelligence (AI), which is widely regarded as a critical pathway toward Artificial General Intelligence (AGI) (Jaech et al., 2024; DeepSeek-AI, 2025). Conventional inference paradigms typically rely on a simple “direct prediction” approach to generate concise final answers without explicit, structured intermediate reasoning steps, which often exhibits suboptimal performance on complex reasoning tasks (Jaech et al., 2024). OpenAI O1 (Jaech et al., 2024) was the first LLM with strong reasoning ability by using complex Chain-of-Thought (CoT) for training to achieve significant performance gains over prior LLMs. Meanwhile, various methods (Wei et al., 2022; Yao et al., 2023; Besta et al., 2024; Lightman et al., 2023; Uesato et al., 2022; Wang et al., 2023; Lai et al., 2024; Wan et al., 2024; Trinh et al., 2024; Xin et al., 2024; Muennighoff et al., 2025; Ye et al., 2025) have been explored to generate high-quality complex CoT reasoning and further advance the field by optimizing reasoning pathways.

In the field of Multimodal Large Language Models (MLLMs), recent works (Yao et al., 2024; Thawakar et al., 2025) have also explored the application of CoT reasoning. These approaches assume that MLLMs lack a structured reasoning process, achieving low performance on the tasks

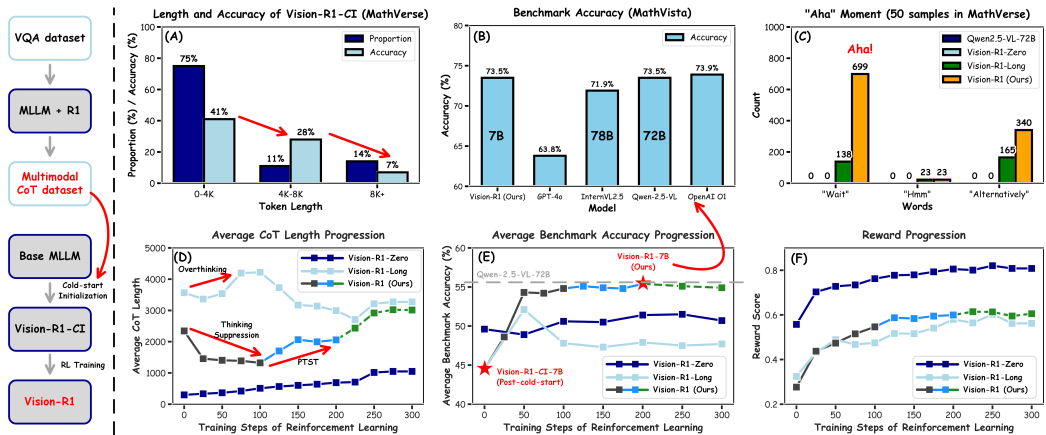


Figure 1: Left panel: Our Vision-R1 Pipeline. We first use the existing MLLM and DeepSeek-R1 to obtain a high-quantity Multimodal CoT dataset, which is used as the cold-start initialization data for the base MLLM to obtain the post-cold-start Vision-R1-CI, and then we perform the RL training on Vision-R1-CI to obtain the reasoning MLLM, Vision-R1. **Right panel:** We observe that directly applying RL to MLLMs fails to effectively incentivize strong reasoning capability (see (C) and (D)). Vision-R1-Zero, trained via RL without prior initialization, struggles to generalize from limited data (see (E), (F), notably, Vision-R1-Zero was applied in format reward function). Vision-R1-CI faces the Overthinking Optimization Problem, favoring shorter CoT reasoning, where correct reasoning processes mostly focus on the shorter CoT reasoning sequences (see (A)). During subsequent RL training, we observe a lengthening of reasoning steps but a decline in performance (see (D) and (E)), making optimization particularly challenging. For Vision-R1, it initially shortens CoT to refine the right thought process under RL training. PTST enables Vision-R1 to progressively acquire a more complex reasoning process (see (C), (D), and (E)) to improve the performance, such that our Vision-R1 with 7B parameters achieves comparable performance to the 70B+ strongest MLLMs (see (B)). Note that Vision-R1 used various colored lines to indicate the different stages in PTST.

that require logical inference. To improve the reasoning capability of MLLMs, several methods (Xu et al., 2024; Yao et al., 2024) try to construct the datasets manually containing step-level reasoning processes and apply supervised fine-tuning (SFT) to reformat MLLMs’ outputs. However, this manually designed “Formatted Reasoning MLLM” often results in “Pseudo-CoT” reasoning, which lacks essential cognitive processes commonly observed in human thoughts, such as questioning, reflection and inspecting (see Fig. 2, the data examples of “Pseudo-CoT” and the complex CoT). This limitation hinders their application on complex vision reasoning tasks. Thus, it is important to generate human-like, high-quality, complex CoT reasoning data for training MLLMs, enabling them to more effectively tackle intricate multimodal reasoning tasks.

Recently, DeepSeek-R1 (DeepSeek-AI, 2025) has successfully applied Reinforcement Learning (RL) to induce the self-emergence of complex cognitive reasoning ability in LLMs. This begs our rethinking: Can RL be utilized to incentivize the reasoning capability in MLLMs? To answer this question, we first follow the DeepSeek-R1-Zero paradigm (DeepSeek-AI, 2025), by directly using RL to improve the reasoning capability of MLLMs. Unfortunately, this direct RL training is challenged, as it struggles to effectively guide MLLMs generating complex CoT reasoning in absence of large-scale, high-quality multimodal data and prolonged training (see Fig. 1 (E) and (F)).

To address the above issue, we propose Vision-R1, a reasoning MLLM that integrates cold-start initialization with RL training. First, we construct a high-quality multimodal CoT dataset without requiring manual annotations. Specifically, we leverage an existing MLLM to generate “Pseudo-CoT” reasoning text from multimodal image-text pairs. This “Pseudo-CoT” reasoning explicitly incorporates both vision descriptions and structured step-level reasoning process, exposing more detailed vision information in a textual format. Next, we feed the enriched reasoning text back into the MLLM to obtain a description including necessary vision information. This process effectively implements “Modality Bridging”, converting vision information to language. The resulting textual descriptions are then passed to a text-only reasoning LLM, DeepSeek-R1, to extract high-quality CoT reasoning. Finally, the dataset is refined through rule-based data filtering, ultimately obtaining

a dataset with 200K multimodal human-like complex CoT reasoning samples, which serves as the cold-start initialization dataset for Vision-R1.

Following the DeepSeek-R1 training pipeline, we need to apply Group Relative Policy Optimization (GRPO) (Shao et al., 2024; DeepSeek-AI, 2025) on a 10K multimodal math dataset to enhance the model’s reasoning capability. However, as shown in Fig. 1 (A) and (D), we observe an overthinking phenomenon in the cold-start initialized MLLM, *i.e.*, the correct reasoning processes tend to be concentrated on shorter CoT reasoning sequences. This issue leads to the optimization problem in subsequent RL training. To address this challenge, we propose Progressive Thinking Suppression Training (PTST) alongside GRPO, which incorporates a hard-formatting result reward function. This approach encourages Vision-R1 to compress CoT reasoning steps early in the RL process, internalizing correct reasoning methods while progressively extending its reasoning duration over time to effectively tackle more complex problems.

Our main contributions can be summarized as follows:

1. We explore how to use R1-like RL for MLLMs and introduce Vision-R1, a reasoning MLLM that leverages cold-start initialization and RL training to incentivize reasoning capability. It is an early exploration that investigates the application of R1-like RL for enhancing reasoning capability in MLLMs and analyzes differences between direct RL training and the combined approach of cold-start initialization and RL training. We believe that our exploration can inspire new insights for the community.
2. A high-quality 200K multimodal CoT dataset without human annotations is constructed to serve as a cold-start initialization data for MLLMs. We leverage the proposed PTST to GRPO with hard-formatting result reward function, which effectively addresses the overthinking optimization problem in RL training. PTST enables Vision-R1 to progressively develop more complex reasoning processes while effectively guiding MLLMs toward enhanced reasoning capability.
3. Notably, despite having only 7B parameters, Vision-R1 achieves performance comparable to State-of-The-Art (SoTA) MLLMs with over 70B parameters in math reasoning tasks. Furthermore, the Vision-R1-32B and Vision-R1-72B models achieve an average accuracy improvement of around 10% compared to the base model on multiple multimodal math benchmarks.

2 RELATED WORK

2.1 LARGE LANGUAGE MODEL REASONING

As researchers have discovered that enabling LLMs to simulate human-like thought processes and perform stepwise reasoning can significantly enhance their performance on reasoning tasks (Jaech et al., 2024), extensive work has been dedicated to exploring LLM reasoning methods. These approaches typically rely on human design to format LLM outputs to follow specific steps, such as Chain-of-Thought (CoT) prompting methods (Wei et al., 2022), plan-based methods like Tree-of-Thought and Graph-of-Thought (Yao et al., 2023; Besta et al., 2024), process-based reward models (Lightman et al., 2023; Uesato et al., 2022; Wang et al., 2023; Lai et al., 2024), Monte Carlo Tree Search (MCTS) and Beam Search (Wan et al., 2024; Trinh et al., 2024; Xin et al., 2024), as well as constructing SFT datasets (Muennighoff et al., 2025; Ye et al., 2025).

A recent development, DeepSeek-R1 (DeepSeek-AI, 2025), demonstrates that applying large-scale Reinforcement Learning (RL) with formatting and result-only reward functions can guide LLMs toward self-emerging thought processes, producing human-like complex CoT reasoning and achieving significant advantages in complex reasoning tasks. This approach has shown immense potential in the field of Large Language Model Reasoning, however, its application to MLLMs remains an open area of inquiry.

2.2 MULTIMODAL LARGE LANGUAGE MODEL REASONING

MLLMs typically map inputs from other modalities to the textual modality, which are then processed by LLMs. This approach has been proven to exhibit superior performance in a range of vision understanding tasks (Liu et al., 2024b;a; Bai et al., 2023; Zhu et al., 2023; Huang et al., 2024; Zhao et al., 2024). Inspired by advancements in LLM reasoning, many studies have also sought

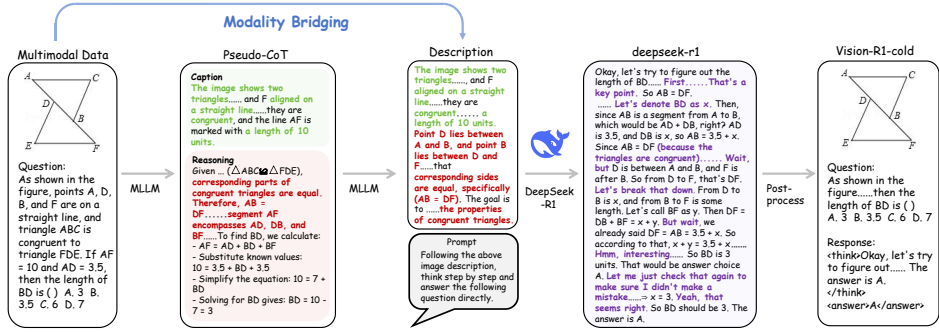


Figure 2: The overall data generation pipeline incorporating our Modality Bridging method. The multimodal data is first sent to MLLMs to obtain a “Pseudo-CoT” consisting of a caption and reasoning process, which serves as the input of MLLMs along with the original image-question pair to produce detailed descriptions. Through this modality bridging approach, the textual descriptions provide DeepSeek-R1 with holistic information that facilitates the generation of high-quality CoT processes, which are post-processed and integrated with the original data to create the final Vision-R1-cold dataset.

to enhance the reasoning capability of MLLMs. For instance, efforts have been made to employ CoT prompting (Zhang et al., 2024b; Mitra et al., 2024; Luan et al., 2024) and to construct SFT datasets that include step-level reasoning (Yao et al., 2024; Thawakar et al., 2025). However, the CoT generated by these methods often lacks natural human cognitive processes, such as questioning, reflection, and inspecting, which limits their effectiveness in solving complex reasoning tasks. In contrast, Vision-R1 distinguishes itself by combining cold-start initialization with RL training to acquire high-quality, complex CoT reasoning capability.

3 METHOD

3.1 CAN ONLY RL INCENTIVIZE REASONING CAPABILITY IN MLLMs?

Inspired by DeepSeek-R1-Zero (DeepSeek-AI, 2025), we aimed to directly use RL to guide models towards self-thought and the emergence of complex reasoning capability. To this end, we collected a dataset of 10K open-source math problems for RL training. Specifically, we followed the DeepSeek-R1-Zero pipeline, training a base MLLM using GRPO (Shao et al., 2024), with output format constraints dictated by the following system prompt:

A conversation between User and Assistant. ... first thinks about the reasoning process ... provides the user with the answer. The reasoning process and answer are enclosed within `<think> </think>` and `<answer> </answer>` tags ...

For the reward function, we utilized both formatting and result rewards:

1. Formatting reward function: The model’s output must adhere to the “`<think> </think><answer> </answer>`” format.
2. Result reward function: The model’s generated final result must align with the ground truth.

We set the formatting and result reward ratio as 1 : 1.

The model after purely RL training is named as Vision-R1-Zero. Unfortunately, as shown in Fig. 1 (D) and (E), directly applying RL to train MLLMs has proven challenging in stimulating MLLM’s reasoning capability and producing lengthy, complex CoT, limiting the model’s reasoning ability. Moreover, we observed that as training progressed over extended periods, the model gradually learned to use longer reasoning processes to solve hard problems, but this did not show significant performance improvement. Thus, we claim that *directly using RL to incentivize the reasoning capability of MLLMs for solving complex reasoning problems remains a challenging task, especially under constraints of data quality and quantity, as well as computation resources.*

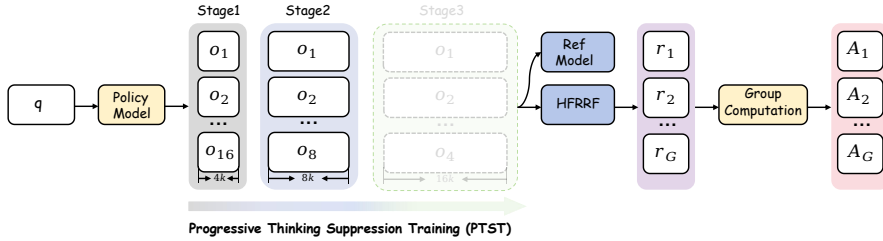


Figure 3: GRPO with our proposed PTST strategy. We progressively loosen the context length restrictions, increasing the length of reasoning process. Specifically, we set the reasoning length to 4K, 8K and 16K tokens for each stage, with corresponding group numbers of 16, 8 and 4 respectively. The reward function for GRPO is based on a hard formatting result reward function (HFRRF). The dotted line in the “Stage 3” indicates that the final version of Vision-R1 did not undergo the third stage of training.

3.2 OVERVIEW OF VISION-R1

In our above explorations, we observed that an RL-only approach struggles to guide MLLMs in generating human-like, complex CoT. Consequently, we explored an alternative strategy and introduced the reasoning MLLM, **Vision-R1**. This method begins with a cold-start using a multimodal CoT dataset, which initially teaches the base model to reason in a “human-like” manner. Subsequently, we apply RL to the cold-start initialized model Vision-R1-CI to guide it towards adopting the correct reasoning process, thereby incentivizing the reasoning capability in the final model Vision-R1.

In the following sections, we first describe our approach to create a high-quality, human annotation-free multimodal CoT dataset in Sec. 3.3.1, as well as the Overthinking Optimization Problem faced by post-cold-start MLLMs in Sec. 3.3.2. Then we discuss the RL training method, Progressive Thinking Suppression Training (PTST) in Sec. 3.4, to address the Overthinking Optimization Problem.

3.3 COLD-START INITIALIZATION

3.3.1 MODALITY BRIDGING TO OBTAIN HIGH-QUALITY MULTIMODAL COT DATA

Many existing works (Xu et al., 2024; Yao et al., 2024) have attempted to construct multimodal reasoning datasets to enhance the reasoning capability of MLLMs. Prior efforts typically gathered CoT data which often lack the natural cognitive processes of questioning, and self-reflection. These datasets are typically constructed in a step-by-step form based on human heuristics. However, our goal is to collect a multimodal CoT dataset that encompasses complex cognitive processes to teach Vision-R1 to reason in a human-like, natural manner. Furthermore, DeepSeek-R1 has demonstrated the ability to generate CoT with natural cognitive processes and has proven to have strong reasoning capability. By using the high-quality CoT data it generates, which incorporates human-like cognitive self-reflection processes, we can train MLLMs to enhance their reasoning capability. However, being a “text-only” LLM, DeepSeek-R1 struggles to effectively process multimodal inputs to produce high-quality CoT.

To overcome these limitations, we utilize existing MLLMs alongside DeepSeek-R1 and propose a method named **Modality Bridging** to indirectly convert multimodal information into textual information, thereby capturing the complex cognitive processes of DeepSeek-R1. As the data generation pipeline that shown in Fig. 2, firstly, we follow prior works (Xu et al., 2024; Yao et al., 2024) by inputting an image-question-answer pair and a prompt into a MLLM to generate a “Pseudo-CoT” featuring both image description and reasoning processes. Subsequently, we concatenate the image-question pair with the “Pseudo-CoT” and a prompt, and then feed them into a MLLM to obtain a detailed image description. Below is the prompt template:

```
Given a image, a question:{question} and a thinking
process:{thinking process}, provide a detailed description
containing all the necessary details of the image to answer the
question correctly...
```

This process of generating “Pseudo-CoT” explicitly exposes more of the necessary vision details for reasoning in textual form, compared to pure image descriptions. This assists the MLLM in producing

Table 1: Comprehensive comparison with SoTA MLLMs (closed-source, open-source general/math/reasoning MLLMs) across diverse multimodal math benchmarks.“Avg.” denotes the average performance over all benchmarks. For MathVista benchmark, we have specifically compared all models on three sub-tasks that are highly related to mathematical reasoning: geometry reasoning (GEO), algebraic reasoning (ALG), geometry problem solving (GPS) and math word problems (MWP). “ALL” denotes the average score on MathVista benchmark. The best results are **bolded**.

Model	Params.	MathVista					MathVerse	MM-Math	DynaMath	Avg.
		GEO	ALG	GPS	MWP	ALL				
<i>Closed-Source MLLMs</i>										
OpenAI O1 (Jaech et al., 2024)	—	—	—	—	—	73.9 [†]	—	—	—	—
GPT-4o (Hurst et al., 2024)	—	—	—	—	—	63.8	37.6	31.8	64.9	—
GPT-4V (OpenAI, 2023)	—	—	—	—	—	49.9	39.4	23.1	—	37.5
Claude-3.5 Sonnet (Anthropic, 2024)	—	—	—	—	—	67.7	26.5	—	62.5	—
<i>Open-Source General MLLMs</i>										
Qwen2.5-VL-7B (Bai et al., 2025)	7B	66.9	68.7	66.8	76.9	68.1	46.7	34.1	50.7	49.9
Qwen2.5-VL-32B (Bai et al., 2025)	32B	72.8	73.7	75.0	72.6	72.9	52.3	34.9	55.5	53.9
Qwen2.5-VL-72B (Bai et al., 2025)	72B	77.8	77.9	78.8	74.7	73.5	51.3	45.6	61.2	57.9
InternVL2.5-78B (Chen et al., 2024c)	78B	76.6	76.5	77.9	75.8	71.9	25.4	17.8	41.4	39.1
<i>Open-Source Math MLLMs</i>										
Math-LLaVA-13B (Shi et al., 2024)	13B	56.5	40.2	57.7	56.5	46.6	22.9	—	—	—
Math-PUMA-Qwen2-7B (Zhuang et al., 2024)	7B	47.3	—	48.1	—	47.9	33.6	—	—	—
Multimath-7B (Peng et al., 2024)	7B	—	—	66.8	61.8	50.0	26.9	—	—	—
URSA-8B (Luo et al., 2025)	8B	—	—	79.3	75.3	59.8	45.7	—	—	—
<i>Open-Source Reasoning MLLMs</i>										
LLaVA-CoT-11B (Xu et al., 2024)	11B	—	—	—	—	54.8	20.3	16.5	34.6	31.6
Mulberry-7B (Yao et al., 2024)	7B	—	—	—	—	63.1	—	23.7	—	—
<i>Our Model</i>										
Vision-R1-7B (Ours)	7B	80.3	79.0	83.2	80.6	73.5	52.4	40.2	56.3	55.6
Δ (vs Qwen2.5-VL-7B)		+13.4	+10.3	+16.4	+3.7	+5.4	+5.7	+6.1	+5.6	+5.7
Vision-R1-32B* (Ours)	32B	85.8	82.6	88.0	78.5	76.4	62.1	55.3	65.6	64.9
Δ (vs Qwen2.5-VL-32B)		+13.0	+8.9	+13.0	+5.9	+4.7	+9.8	+20.4	+10.1	+11.0
Vision-R1-72B* (Ours)	72B	88.3	86.8	89.4	79.6	78.2	63.2	59.3	66.4	66.8
Δ (vs Qwen2.5-VL-72B)		+10.5	+8.9	+10.6	+4.9	+4.7	+11.9	+13.7	+5.2	+8.9

[†] The result is collected from the official MathVista leaderboard (<https://mathvista.github.io/#leaderboard>).

* It uses additional data during RL training.

more detailed descriptions, thereby minimizing information loss during the conversion of original multimodal information to textual information (see Fig. 5).

At this stage, we cleverly bridge image information to textual information and feed it into DeepSeek-R1 to obtain high-quality CoT processes. We then retain reasoning processes from the generated multimodal CoT data that the final answer is aligned with ground truth and apply rule-based data filtering to remove logical inconsistent samples and replace some words for semantic coherence.

Finally, we pair the pure text CoT data generated by DeepSeek-R1 from the above process with the corresponding images, integrating into multimodal CoT data, named **Vision-R1-cold** dataset. This dataset is used for the cold-start initialization of Vision-R1. By acquiring CoT data in this manner, which closely mimics human cognitive behavior, the reasoning processes exhibit natural thinking.

3.3.2 OVERTHINKING OPTIMIZATION PROBLEM

After obtaining a multimodal CoT dataset, we conducted SFT on a pretrained MLLM (such as Qwen2.5-VL (Bai et al., 2025)) as the base MLLM for cold-start initialization. The MLLM after cold start initialization is named as Vision-R1-CI. At this stage, the base MLLM had learned the complex reasoning mode from DeepSeek-R1, however, this led to the Overthinking Optimization Problem, *i.e.*, Vision-R1-CI would engage in prolonged thought processes on certain problems, whereas the correct reasoning processes were typically concentrated in shorter cognitive chains.

As shown in Fig. 1 (D) and (E), this propensity for excessive incorrect reasoning significantly complicates the optimization of subsequent RL training. For instance, when the allowed thought length during RL training for Vision-R1-CI was directly extended to 16K, the model tended to generate longer answers to fulfill the demands of complex reasoning. However, this incorrect reasoning did not lead to performance improvements, thus presenting challenges in incentivizing reasoning capability in MLLMs. So, *it is crucial to guide the model to learn correct thinking in the early stages for the reasoning performance of MLLMs*.

Table 2: Comparison with SoTA MLLMs across diverse comprehensive multimodal benchmarks. The base MLLM is Llama-3.2-11B-V-Instruct (Dubey et al., 2024). The results indicate that our data significantly enhances the generalization capabilities of our model, leading to superior performance across all benchmarks.

Method	General Benchmark				Math Benchmark		
	MMStar	ChartQA	MME _{sum}	HallBench	MathVista	MathVerse	MM-Math
Llama-3.2-11B-V (Dubey et al., 2024)	49.8	83.4	1787	40.3	48.6	8.4	4.1
Mulberry-Llama-11B (Yao et al., 2024)	58.5	83.5	2035	48.9	61.1	—	18.7
LLaVA-Cot-11B (Xu et al., 2024)	57.6	81.9	2137	47.8	54.8	20.3	16.5
Vision-R1-LlamaV-CI-11B	61.4	83.9	2190	49.5	62.7	27.1	26.1

3.4 PROGRESSIVE THINKING SUPPRESSION TRAINING

Inspired by the above phenomenon, we propose the Progressive Thinking Suppression Training (PTST) algorithm to initially suppress the length of reasoning during the early stages of RL training for Vision-R1, while guiding it towards the correct reasoning processes. As training progresses, we gradually relax these constraints, allowing Vision-R1 to autonomously learn to utilize longer CoT to address increasingly complex problems, thereby enhancing its reasoning capability. Specifically, we implement Group Relative Policy Optimization (GRPO) with hard formatting result rewards for the model’s self-learning. Consider the standard GRPO approach, it samples a group of generated output set $\{o_1, o_2, \dots, o_G\}$ for each question q from policy model $\pi_{\theta_{old}}$. Then GRPO maximizes the following objective and optimizes the model π_{θ} .

$$J_{\text{GRPO}}(\theta) = \mathbb{E}_{q \sim P(Q), \{o_i\}_{i=1}^G \sim \pi_{\theta_{old}}(O|q)} \left[\frac{1}{G} \sum_{i=1}^G \min\left(\frac{\pi_{\theta}(o_i | q)}{\pi_{\theta_{old}}(o_i | q)} A_i, \text{clip}\left(\frac{\pi_{\theta}(o_i | q)}{\pi_{\theta_{old}}(o_i | q)}, 1 - \varepsilon, 1 + \varepsilon\right) A_i\right) - \beta D_{\text{KL}}(\pi_{\theta} \| \pi_{\text{ref}}) \right], \quad (1)$$

where ε and β are the PPO clipping hyper-parameter and the coefficient controlling the Kullback–Leibler (KL) penalty (Shao et al., 2024; Schulman et al., 2017), respectively. We set $\varepsilon=0.2$ and $\beta=1e-2$ during training. $A_i = \frac{r_i - \text{mean}(\{r_1, r_2, \dots, r_G\})}{\text{std}(\{r_1, r_2, \dots, r_G\})}$ is the computed advantage using the group rewards $\{r_1, r_2, \dots, r_G\}$ and $D_{KL}(\pi_{\theta} \| \pi_{\text{ref}}) = \frac{\pi_{\text{ref}}(o_i | q)}{\pi_{\theta}(o_i | q)} - \log\left(\frac{\pi_{\text{ref}}(o_i | q)}{\pi_{\theta}(o_i | q)}\right) - 1$ is the KL divergence.

As shown in Fig. 3, in our proposed PTST, we denote the total number of training stages by S , with each stage having its own sampling count G_s and sequence length limit L_s . The output space for stage $s \in \{1, 2, \dots, S\}$ is $O^{(s)} = \{o : |o| \leq L_s\}$. The training objective for the s -th stage can be further reformulated based on Eq. 1 as:

$$J_{\text{GRPO}}^{(s), \text{w/PTST}}(\theta) = \mathbb{E}_{q \sim P(Q), \{o_i^{(s)}\}_{i=1}^{G_s} \sim \pi_{\theta_{old}}(O^{(s)}|q)} \left[\frac{1}{G_s} \sum_{i=1}^{G_s} \min\left(\frac{\pi_{\theta}(o_i^{(s)} | q)}{\pi_{\theta_{old}}(o_i^{(s)} | q)} A_i^{(s)}, \text{clip}\left(\frac{\pi_{\theta}(o_i^{(s)} | q)}{\pi_{\theta_{old}}(o_i^{(s)} | q)}, 1 - \varepsilon, 1 + \varepsilon\right) A_i^{(s)}\right) - \beta D_{\text{KL}}(\pi_{\theta} \| \pi_{\text{ref}}) \right], \quad (2)$$

where $A_i^{(s)}$ denotes the advantage estimate for the i -th sample in the training stage s , and $\pi_{\theta_{old}}$ denotes the policy model with an output length constraint of $O(s)$. We employ the hard formatting result reward function as the reward mechanism for GRPO, *i.e.*, the model receives a reward score of $r_i = 1$ only when both the formatting requirements and the correctness of the final answer are simultaneously satisfied; otherwise, it receives a score of $r_i = 0$. Moreover, we do not impose constraints using a system prompt, as Vision-R1-CI has already acquired robust formatting capability during the cold-start initialization.

By applying PTST, we compress the model’s thought length in the early training stages to guide correct reasoning and gradually relax these constraints in later stages. As illustrated in Fig. 1, this progressive strategy enables Vision-R1 to generate more complex CoT and significantly enhances its reasoning capability. Notably, in practice, we observe that Vision-R1 achieves competitive performance by the end of the second training stage, leading us to select it as the final stage, *i.e.*, we set the parameters as $S = 2$, $L_s \in \{4K, 8K, 16K\}$, and $G_s \in \{16, 8, 4\}$, respectively.

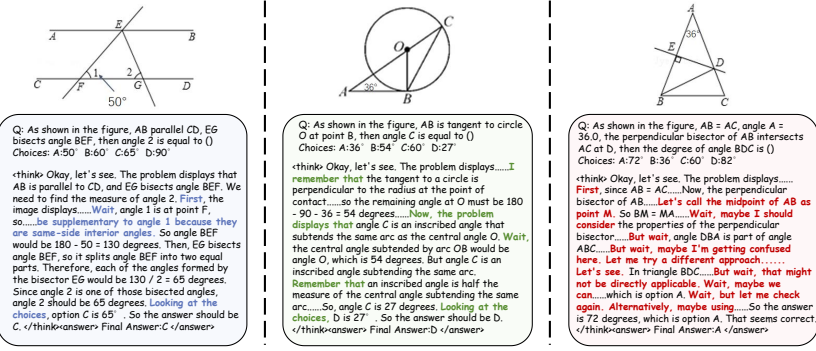


Figure 4: The output examples of Vision-R1-7B on MathVerse benchmark. Vision-R1-7B shows “human-like” questioning and self-reflective thought process when solving math reasoning problems, which is also called “*Aha moment*” in DeepSeek-R1’s paper (DeepSeek-AI, 2025). More examples are provided in supplementary materials.

4 EXPERIMENTS

Please refer to Appendix A to obtain the detailed data and training settings. We provide the main results of Vision-R1 in Sec 4.1, and then we introduce the detailed ablation study in Sec 4.2.

4.1 MAIN RESULTS

As shown in Tab. 1, our proposed Vision-R1-7B achieves competitive results across multiple math reasoning benchmarks, even when compared to SoTA models with over 10 times the parameters of Vision-R1-7B. For instance, on the MathVista benchmark, Vision-R1-7B achieves a score of 73.5%, only 0.4% lower than OpenAI O1, the most widely recognized reasoning model.

Table 3: Evaluating the impact of Cold Start Initialization, GRPO, Progressive Thinking Suppression Training (PTST). “Avg. Len.” denotes the average output token length on the 10K multimodal math dataset for RL training. “Avg. Acc.” denotes the average performance (MathVista, MathVerse, MM-Math).

Method	Cold Start	GRPO	PTST	Avg. Len.	Avg. Acc.
Vision-R1-Zero		✓		1285	50.7
Vision-R1-CI	✓			3566	44.5
Vision-R1-Long	✓	✓		3107	47.7
Vision-R1 (Ours)	✓	✓	✓	2057	55.4

ter being second only to Qwen-2.5-VL-72B. This demonstrates Vision-R1-7B’s effectiveness in solving complex math problems.

4.2 ABLATION STUDY

Cold-start Dataset Quality. We conduct a quality analysis of our proposed Vision-R1-cold dataset. The primary objective of constructing Vision-R1-cold is to supplement the existing multimodal CoT datasets, which lack complex cognitive processes, and to leverage DeepSeek-R1’s high-quality CoT process as cold-start data. To evaluate this, we present a comparative analysis in Tab. 4, where we statistically examine the presence of questioning, reflection, and inspection within the CoT processes of Mulberry, LLaVA-CoT, and Vision-R1-cold datasets. The results indicate that Vision-R1-cold contains a significantly higher proportion of human-like cognitive processes compared to previous multimodal CoT datasets. This complex CoT structure facilitates the base MLLM in learning reasoning mechanisms, providing a high-quality cold-start initialization for RL training.

Additionally, we compare Vision-R1-cold with previous multimodal CoT datasets by training on Llama-3.2-11B-V in Tab. 2. After SFT, our Vision-R1-LlamaV-CI-11B model achieves SoTA

Table 4: Comparison of the occurrence frequency of self-reflective indicators between llava-cot, mulberry and our Vision-R1-cold dataset. The higher frequency of these reflective markers in our dataset demonstrates its distinctive self-reflection and self-correction characteristic.

Word	llava-cot (100K)	Mulberry (260K)	Vision-R1-cold (200K)
“Wait”	2,300	1,122	585,719
“Hmm”	1	0	75,853
“Mistake”	183	8,784	26,697
“Alternatively”	251	68	188,187
“Check”	8,332	26,421	100,148

Table 5: Effect of PTST. “ $4K \times 16$ ” denotes a PTST setup where the Stage limits the response length to 4K with 16 samples. “Avg.” denotes the average performance (MathVista, MathVerse, MM-Math).

Method	Stage 1	Stage 2	Stage 3	MathVisita	MathVerse	MM-Math	Avg.
Baseline	—	—	—	68.1	46.7	34.1	49.6
—	$4K \times 16$	$4K \times 16$	—	72.6	51.4	39.0	54.3
—	$4K \times 16$	$8K \times 16$	—	72.9	53.5	39.5	55.3
—	$4K \times 16$	$6K \times 12$	$8K \times 8$	73.0	52.6	39.8	55.1
Vision-R1-Long	$16K \times 4$	$16K \times 4$	—	70.3	36.8	36.1	47.7
—	$16K \times 16$	$16K \times 16$	—	71.1	36.5	36.1	47.9
Vision-R1 (Ours)	$4K \times 16$	$8K \times 8$	—	73.5	52.4	40.2	55.4

performance across all general and math reasoning benchmarks, outperforming both LLaVA-CoT-11B and Mulberry-Llama-11B, directly confirming the superior quality of Vision-R1-cold dataset.

Effect of Main Strategy. As shown in Tab. 3, we compare the performance of various RL training strategies. The results indicate that Vision-R1-Zero, which applies RL training directly without cold-start initialization, struggles to generate sufficiently long and complex CoT reasoning, thereby limiting its ability to handle intricate reasoning tasks. In contrast, Vision-R1-CI, after cold-start initialization, tends to generate excessively long CoTs. However, the presence of numerous incorrect reasoning steps leads to lower overall performance. Furthermore, Vision-R1-Long via applying RL training directly to Vision-R1-CI results in optimization difficulty, making it hard to achieve significant performance improvements. In comparison, our proposed Vision-R1 demonstrates a substantial advantage in reasoning performance, effectively balancing CoT complexity and accuracy.

Effect of PTST. In Tab. 5, our two-stage setup ($4K \times 16 \rightarrow 8K \times 8$) achieves the best average (55.4%), outperforming training with a fixed short length ($4K \times 16 \rightarrow 4K \times 16$) by +1.1 Avg. (54.3 → 55.4), indicating that progressively relaxing the length constraint in Stage 2 yields consistent gains once correct thinking is established in Stage 1. In contrast, training with fixed 16K ($16K \times 4$ or $16K \times 16$) severely underperforms (47.7%/47.9%), showing that early length constraints effectively mitigate overthinking. Further increasing Stage 2 sampling to 16 ($4K \times 16 \rightarrow 8K \times 16$, 55.3%) or inserting an extra stage ($4K \times 16 \rightarrow 6K \times 12 \rightarrow 8K \times 8$, 55.1%) brings no meaningful improvement, suggesting PTST is robust and a simple two-stage schedule suffices under matched training time (sampling × length kept constant per stage).

Effect of Cold Start. Tab. 6 demonstrates that PTST alone offers limited benefit without cold start (Zero+PTST: 51.8% vs Vision-R1-Zero: 50.7%), and SFT without CoT before RL is detrimental (Zero+SFT+PTST: 39.8%). In contrast, cold-starting on Vision-R1-cold followed by PTST yields the best average (55.4%), with a substantial gain on MM-Math (40.2% vs 33.1%/28.8%). These results support that complex CoT priors acquired in cold start are essential for RL to learn correct reasoning patterns. Furthermore, PTST then suppresses early overthinking (short 4K) and safely extends reasoning length (8K), leading to consistent improvements.

Visualization. As shown in Fig. 4, our proposed Vision-R1-7B is capable of generating complex reasoning processes and exhibits the emergence of the so-called “Aha moment” (DeepSeek-AI, 2025), *i.e.*, a phenomenon analogous to human cognitive processes involving questioning and reflection. This sophisticated reasoning capability significantly enhances the model’s inference performance, leading to substantial improvements in solving complex reasoning tasks.

Table 6: Effect of Cold Start. “Zero+PTST” denotes we keep the Vision-R1-Zero settings while adopting PTST strategy. “Zero+SFT+PTST” involves training the base model in the Vision-R1-cold dataset *without CoT annotations* before RL training, followed by RL training with the same “Zero+PTST” setup. “Avg.” denotes the average performance (MathVista, MathVerse, MM-Math).

Method	MathVisita	MathVerse	MM-Math	Avg.
Vision-R1-Zero	70.6	52.6	28.8	50.7
Zero+PTST	71.3	50.9	33.1	51.8
Zero+SFT+PTST	68.7	32.0	18.9	39.8
Vision-R1 (Ours)	73.5	52.4	40.2	55.4

5 CONCLUSION

We explore how to use RL training to incentivize reasoning capability in MLLMs. Moreover, we proposed Vision-R1 and achieved the strong math reasoning ability, achieving comparable performance to SoTA MLLMs.

REFERENCES

Anthropic. Claude 3.5 sonnet. <https://www.anthropic.com/news/claude-3-5-sonnet>, 2024.

Stanislaw Antol, Aishwarya Agrawal, Jiasen Lu, Margaret Mitchell, Dhruv Batra, C Lawrence Zitnick, and Devi Parikh. Vqa: Visual question answering. In *Proceedings of the IEEE international conference on computer vision*, pp. 2425–2433, 2015.

Jinze Bai, Shuai Bai, Shusheng Yang, Shijie Wang, Sinan Tan, Peng Wang, Junyang Lin, Chang Zhou, and Jingren Zhou. Qwen-vl: A frontier large vision-language model with versatile abilities. *arXiv preprint arXiv:2308.12966*, 2023.

Shuai Bai, Keqin Chen, Xuejing Liu, Jialin Wang, Wenbin Ge, Sibo Song, Kai Dang, Peng Wang, Shijie Wang, Jun Tang, Humen Zhong, Yuanzhi Zhu, Mingkun Yang, Zhaohai Li, Jianqiang Wan, Pengfei Wang, Wei Ding, Zheren Fu, Yiheng Xu, Jiabo Ye, Xi Zhang, Tianbao Xie, Zesen Cheng, Hang Zhang, Zhibo Yang, Haiyang Xu, and Junyang Lin. Qwen2.5-vl technical report. *arXiv preprint arXiv:2502.13923*, 2025.

Maciej Besta, Nils Blach, Ales Kubicek, Robert Gerstenberger, Michal Podstawski, Lukas Gianinazzi, Joanna Gajda, Tomasz Lehmann, Hubert Niewiadomski, Piotr Nyczek, et al. Graph of thoughts: Solving elaborate problems with large language models. In *Proceedings of the AAAI Conference on Artificial Intelligence*, volume 38, pp. 17682–17690, 2024.

Huanqia Cai, Yijun Yang, and Winston Hu. Mm-iq: Benchmarking human-like abstraction and reasoning in multimodal models. *arXiv preprint arXiv:2502.00698*, 2025.

Jie Cao and Jing Xiao. An augmented benchmark dataset for geometric question answering through dual parallel text encoding. In *Proceedings of the 29th international conference on computational linguistics*, pp. 1511–1520, 2022.

Jiaqi Chen, Jianheng Tang, Jinghui Qin, Xiaodan Liang, Lingbo Liu, Eric P Xing, and Liang Lin. Geoqa: A geometric question answering benchmark towards multimodal numerical reasoning. *arXiv preprint arXiv:2105.14517*, 2021.

Jiaqi Chen, Tong Li, Jinghui Qin, Pan Lu, Liang Lin, Chongyu Chen, and Xiaodan Liang. Unigeo: Unifying geometry logical reasoning via reformulating mathematical expression. *arXiv preprint arXiv:2212.02746*, 2022.

Lin Chen, Jinsong Li, Xiaoyi Dong, Pan Zhang, Conghui He, Jiaqi Wang, Feng Zhao, and Dahua Lin. Sharegpt4v: Improving large multi-modal models with better captions. In *European Conference on Computer Vision*, pp. 370–387. Springer, 2024a.

Lin Chen, Jinsong Li, Xiaoyi Dong, Pan Zhang, Yuhang Zang, Zehui Chen, Haodong Duan, Jiaqi Wang, Yu Qiao, Dahua Lin, et al. Are we on the right way for evaluating large vision-language models? *arXiv preprint arXiv:2403.20330*, 2024b.

Zhe Chen, Weiyun Wang, Yue Cao, Yangzhou Liu, Zhangwei Gao, Erfei Cui, Jinguo Zhu, Shenglong Ye, Hao Tian, Zhaoyang Liu, et al. Expanding performance boundaries of open-source multimodal models with model, data, and test-time scaling. *arXiv preprint arXiv:2412.05271*, 2024c.

DeepSeek-AI. Deepseek-rl: Incentivizing reasoning capability in llms via reinforcement learning, 2025. URL <https://arxiv.org/abs/2501.12948>.

Abhimanyu Dubey, Abhinav Jauhri, Abhinav Pandey, Abhishek Kadian, Ahmad Al-Dahle, Aiesha Letman, Akhil Mathur, Alan Schelten, Amy Yang, Angela Fan, et al. The llama 3 herd of models. *arXiv preprint arXiv:2407.21783*, 2024.

Chaoyou Fu, Peixian Chen, Yunhang Shen, Yulei Qin, Mengdan Zhang, Xu Lin, Zhenyu Qiu, Wei Lin, Jinrui Yang, Xiawu Zheng, Ke Li, Xing Sun, and Rongrong Ji. Mme: A comprehensive evaluation benchmark for multimodal large language models. *ArXiv*, abs/2306.13394, 2023. URL <https://api.semanticscholar.org/CorpusID:259243928>.

Jiahui Gao, Renjie Pi, Jipeng Zhang, Jiacheng Ye, Wanjun Zhong, Yufei Wang, Lanqing Hong, Jianhua Han, Hang Xu, Zhenguo Li, et al. G-llava: Solving geometric problem with multi-modal large language model. *arXiv preprint arXiv:2312.11370*, 2023.

Yash Goyal, Tejas Khot, Douglas Summers-Stay, Dhruv Batra, and Devi Parikh. Making the v in vqa matter: Elevating the role of image understanding in visual question answering. In *Proceedings of the IEEE conference on computer vision and pattern recognition*, pp. 6904–6913, 2017.

Tianrui Guan, Fuxiao Liu, Xiyang Wu, Ruiqi Xian, Zongxia Li, Xiaoyu Liu, Xijun Wang, Lichang Chen, Furong Huang, Yaser Yacoob, et al. Hallusionbench: an advanced diagnostic suite for entangled language hallucination and visual illusion in large vision-language models. In *Proceedings of the IEEE/CVF Conference on Computer Vision and Pattern Recognition*, pp. 14375–14385, 2024.

Jarvis Guo, Tuney Zheng, Yuelin Bai, Bo Li, Yubo Wang, King Zhu, Yizhi Li, Graham Neubig, Wenhui Chen, and Xiang Yue. Mammoth-vl: Eliciting multimodal reasoning with instruction tuning at scale. *arXiv preprint arXiv:2412.05237*, 2024.

Himanshu Gupta, Shreyas Verma, Ujjwala Anantheswaran, Kevin Scaria, Mihir Parmar, Swaroop Mishra, and Chitta Baral. Polymath: A challenging multi-modal mathematical reasoning benchmark. *arXiv preprint arXiv:2410.14702*, 2024.

Danna Gurari, Qing Li, Abigale J Stangl, Anhong Guo, Chi Lin, Kristen Grauman, Jiebo Luo, and Jeffrey P Bigham. Vizwiz grand challenge: Answering visual questions from blind people. In *Proceedings of the IEEE conference on computer vision and pattern recognition*, pp. 3608–3617, 2018.

Wenxuan Huang, Zijie Zhai, Yunhang Shen, Shaoshen Cao, Fei Zhao, Xiangfeng Xu, Zheyu Ye, and Shaohui Lin. Dynamic-llava: Efficient multimodal large language models via dynamic vision-language context sparsification. *arXiv preprint arXiv:2412.00876*, 2024.

Aaron Hurst, Adam Lerer, Adam P Goucher, Adam Perelman, Aditya Ramesh, Aidan Clark, AJ Os-trow, Akila Welihinda, Alan Hayes, Alec Radford, et al. Gpt-4o system card. *arXiv preprint arXiv:2410.21276*, 2024.

Aaron Jaech, Adam Kalai, Adam Lerer, Adam Richardson, Ahmed El-Kishky, Aiden Low, Alec Helyar, Aleksander Madry, Alex Beutel, Alex Carney, et al. Openai o1 system card. *arXiv preprint arXiv:2412.16720*, 2024.

Justin Johnson, Bharath Hariharan, Laurens Van Der Maaten, Li Fei-Fei, C Lawrence Zitnick, and Ross Girshick. Clevr: A diagnostic dataset for compositional language and elementary visual reasoning. In *Proceedings of the IEEE conference on computer vision and pattern recognition*, pp. 2901–2910, 2017.

Kushal Kafle, Brian Price, Scott Cohen, and Christopher Kanan. Dvqa: Understanding data visualizations via question answering. In *Proceedings of the IEEE conference on computer vision and pattern recognition*, pp. 5648–5656, 2018.

Samira Ebrahimi Kahou, Vincent Michalski, Adam Atkinson, Ákos Kádár, Adam Trischler, and Yoshua Bengio. Figureqa: An annotated figure dataset for visual reasoning. *arXiv preprint arXiv:1710.07300*, 2017.

Mehran Kazemi, Hamidreza Alvari, Ankit Anand, Jialin Wu, Xi Chen, and Radu Soricut. Geomverse: A systematic evaluation of large models for geometric reasoning. *arXiv preprint arXiv:2312.12241*, 2023.

Aniruddha Kembhavi, Mike Salvato, Eric Kolve, Minjoon Seo, Hannaneh Hajishirzi, and Ali Farhadi. A diagram is worth a dozen images. In *Computer Vision–ECCV 2016: 14th European Conference, Amsterdam, The Netherlands, October 11–14, 2016, Proceedings, Part IV 14*, pp. 235–251. Springer, 2016.

Aniruddha Kembhavi, Minjoon Seo, Dustin Schwenk, Jonghyun Choi, Ali Farhadi, and Hannaneh Hajishirzi. Are you smarter than a sixth grader? textbook question answering for multimodal machine comprehension. In *Proceedings of the IEEE Conference on Computer Vision and Pattern Recognition*, pp. 4999–5007, 2017.

Xin Lai, Zhuotao Tian, Yukang Chen, Senqiao Yang, Xiangru Peng, and Jiaya Jia. Step-dpo: Step-wise preference optimization for long-chain reasoning of llms. *arXiv preprint arXiv:2406.18629*, 2024.

Jason J Lau, Soumya Gayen, Asma Ben Abacha, and Dina Demner-Fushman. A dataset of clinically generated visual questions and answers about radiology images. *Scientific data*, 5(1):1–10, 2018.

Junnan Li, Yongkang Wong, Qi Zhao, and Mohan S Kankanhalli. Dual-glance model for deciphering social relationships. In *Proceedings of the IEEE international conference on computer vision*, pp. 2650–2659, 2017.

Zhuowan Li, Xingrui Wang, Elias Stengel-Eskin, Adam Kortylewski, Wufei Ma, Benjamin Van Durme, and Alan L Yuille. Super-clevr: A virtual benchmark to diagnose domain robustness in visual reasoning. In *Proceedings of the IEEE/CVF conference on computer vision and pattern recognition*, pp. 14963–14973, 2023.

Zhenwen Liang, Kehan Guo, Gang Liu, Taicheng Guo, Yujun Zhou, Tianyu Yang, Jiajun Jiao, Renjie Pi, Jipeng Zhang, and Xiangliang Zhang. Scemqa: A scientific college entrance level multimodal question answering benchmark. *arXiv preprint arXiv:2402.05138*, 2024.

Hunter Lightman, Vineet Kosaraju, Yuri Burda, Harrison Edwards, Bowen Baker, Teddy Lee, Jan Leike, John Schulman, Ilya Sutskever, and Karl Cobbe. Let’s verify step by step. In *The Twelfth International Conference on Learning Representations*, 2023.

Adam Dahlgren Lindström and Savitha Sam Abraham. Clevr-math: A dataset for compositional language, visual and mathematical reasoning. *arXiv preprint arXiv:2208.05358*, 2022.

Fuxiao Liu, Kevin Lin, Linjie Li, Jianfeng Wang, Yaser Yacoob, and Lijuan Wang. Mitigating hallucination in large multi-modal models via robust instruction tuning. *arXiv preprint arXiv:2306.14565*, 2023.

Haotian Liu, Chunyuan Li, Yuheng Li, and Yong Jae Lee. Improved baselines with visual instruction tuning. In *Proceedings of the IEEE/CVF Conference on Computer Vision and Pattern Recognition*, pp. 26296–26306, 2024a.

Haotian Liu, Chunyuan Li, Qingyang Wu, and Yong Jae Lee. Visual instruction tuning. *Advances in neural information processing systems*, 36, 2024b.

Pan Lu, Ran Gong, Shibiao Jiang, Liang Qiu, Siyuan Huang, Xiaodan Liang, and Song-Chun Zhu. Inter-gps: Interpretable geometry problem solving with formal language and symbolic reasoning. *arXiv preprint arXiv:2105.04165*, 2021a.

Pan Lu, Liang Qiu, Jiaqi Chen, Tony Xia, Yizhou Zhao, Wei Zhang, Zhou Yu, Xiaodan Liang, and Song-Chun Zhu. Iconqa: A new benchmark for abstract diagram understanding and visual language reasoning. *arXiv preprint arXiv:2110.13214*, 2021b.

Pan Lu, Swaroop Mishra, Tanglin Xia, Liang Qiu, Kai-Wei Chang, Song-Chun Zhu, Oyvind Tafjord, Peter Clark, and Ashwin Kalyan. Learn to explain: Multimodal reasoning via thought chains for science question answering. *Advances in Neural Information Processing Systems*, 35:2507–2521, 2022.

Pan Lu, Hritik Bansal, Tony Xia, Jiacheng Liu, Chunyuan Li, Hannaneh Hajishirzi, Hao Cheng, Kai-Wei Chang, Michel Galley, and Jianfeng Gao. Mathvista: Evaluating mathematical reasoning of foundation models in visual contexts. *arXiv preprint arXiv:2310.02255*, 2023a.

Pan Lu, Liang Qiu, Kai-Wei Chang, Ying Nian Wu, Song-Chun Zhu, Tanmay Rajpurohit, Peter Clark, and Ashwin Kalyan. Dynamic prompt learning via policy gradient for semi-structured mathematical reasoning. In *International Conference on Learning Representations (ICLR)*, 2023b.

Bozhi Luan, Hao Feng, Hong Chen, Yonghui Wang, Wengang Zhou, and Houqiang Li. Textcot: Zoom in for enhanced multimodal text-rich image understanding. *arXiv preprint arXiv:2404.09797*, 2024.

Ruilin Luo, Zhuofan Zheng, Yifan Wang, Yiyao Yu, Xinzhe Ni, Zicheng Lin, Jin Zeng, and Yujiu Yang. Ursu: Understanding and verifying chain-of-thought reasoning in multimodal mathematics. *arXiv preprint arXiv:2501.04686*, 2025.

Ahmed Masry, Do Xuan Long, Jia Qing Tan, Shafiq Joty, and Enamul Hoque. Chartqa: A benchmark for question answering about charts with visual and logical reasoning. *arXiv preprint arXiv:2203.10244*, 2022.

Minesh Mathew, Dimosthenis Karatzas, and CV Jawahar. Docvqa: A dataset for vqa on document images. In *Proceedings of the IEEE/CVF winter conference on applications of computer vision*, pp. 2200–2209, 2021.

Minesh Mathew, Viraj Bagal, Rubèn Tito, Dimosthenis Karatzas, Ernest Valveny, and CV Jawahar. Infographicvqa. In *Proceedings of the IEEE/CVF Winter Conference on Applications of Computer Vision*, pp. 1697–1706, 2022.

Nitesh Methani, Pritha Ganguly, Mitesh M Khapra, and Pratyush Kumar. Plotqa: Reasoning over scientific plots. In *Proceedings of the IEEE/CVF Winter Conference on Applications of Computer Vision*, pp. 1527–1536, 2020.

Chanchalik Mitra, Brandon Huang, Trevor Darrell, and Roei Herzig. Compositional chain-of-thought prompting for large multimodal models. In *Proceedings of the IEEE/CVF Conference on Computer Vision and Pattern Recognition*, pp. 14420–14431, 2024.

Niklas Muennighoff, Zitong Yang, Weijia Shi, Xiang Lisa Li, Li Fei-Fei, Hannaneh Hajishirzi, Luke Zettlemoyer, Percy Liang, Emmanuel Candès, and Tatsunori Hashimoto. s1: Simple test-time scaling. *arXiv preprint arXiv:2501.19393*, 2025.

OpenAI. Gpt-4v(ision) system card. <https://openai.com/index/gpt-4v-system-card>, 2023.

Shuai Peng, Di Fu, Liangcai Gao, Xiuqin Zhong, Hongguang Fu, and Zhi Tang. Multimath: Bridging visual and mathematical reasoning for large language models. *arXiv preprint arXiv:2409.00147*, 2024.

Runqi Qiao, Qiuna Tan, Guanting Dong, Minhui Wu, Chong Sun, Xiaoshuai Song, Zhuoma GongQue, Shanglin Lei, Zhe Wei, MiaoXuan Zhang, et al. We-math: Does your large multimodal model achieve human-like mathematical reasoning? *arXiv preprint arXiv:2407.01284*, 2024.

John Schulman, Filip Wolski, Prafulla Dhariwal, Alec Radford, and Oleg Klimov. Proximal policy optimization algorithms. *arXiv preprint arXiv:1707.06347*, 2017.

Dustin Schwenk, Apoorv Khandelwal, Christopher Clark, Kenneth Marino, and Roozbeh Mottaghi. A-okvqa: A benchmark for visual question answering using world knowledge. In *European conference on computer vision*, pp. 146–162. Springer, 2022.

Minjoon Seo, Hannaneh Hajishirzi, Ali Farhadi, Oren Etzioni, and Clint Malcolm. Solving geometry problems: Combining text and diagram interpretation. In *Proceedings of the 2015 conference on empirical methods in natural language processing*, pp. 1466–1476, 2015.

Zhihong Shao, Peiyi Wang, Qihao Zhu, Runxin Xu, Junxiao Song, Xiao Bi, Haowei Zhang, Mingchuan Zhang, YK Li, Y Wu, et al. Deepseekmath: Pushing the limits of mathematical reasoning in open language models. *arXiv preprint arXiv:2402.03300*, 2024.

Guangming Sheng, Chi Zhang, Zilingfeng Ye, Xibin Wu, Wang Zhang, Ru Zhang, Yanghua Peng, Haibin Lin, and Chuan Wu. Hybridflow: A flexible and efficient rlhf framework. *arXiv preprint arXiv: 2409.19256*, 2024.

Wenhao Shi, Zhiqiang Hu, Yi Bin, Junhua Liu, Yang Yang, See-Kiong Ng, Lidong Bing, and Roy Ka-Wei Lee. Math-LLaVA: Bootstrapping mathematical reasoning for multimodal large language models. In *Findings of the Association for Computational Linguistics: EMNLP 2024*, pp. 4663–4680, November 2024.

Amanpreet Singh, Vivek Natarajan, Meet Shah, Yu Jiang, Xinlei Chen, Dhruv Batra, Devi Parikh, and Marcus Rohrbach. Towards vqa models that can read. In *Proceedings of the IEEE/CVF conference on computer vision and pattern recognition*, pp. 8317–8326, 2019.

Kai Sun, Yushi Bai, Ji Qi, Lei Hou, and Juanzi Li. Mm-math: Advancing multimodal math evaluation with process evaluation and fine-grained classification. *arXiv preprint arXiv:2404.05091*, 2024.

Omkar Thawakar, Dinura Dissanayake, Ketan More, Ritesh Thawkar, Ahmed Heakl, Noor Ahsan, Yuhao Li, Mohammed Zumri, Jean Lahoud, Rao Muhammad Anwer, et al. Llamav-o1: Rethinking step-by-step visual reasoning in llms. *arXiv preprint arXiv:2501.06186*, 2025.

Trieu H Trinh, Yuhuai Wu, Quoc V Le, He He, and Thang Luong. Solving olympiad geometry without human demonstrations. *Nature*, 625(7995):476–482, 2024.

Jonathan Uesato, Nate Kushman, Ramana Kumar, Francis Song, Noah Siegel, Lisa Wang, Antonia Creswell, Geoffrey Irving, and Irina Higgins. Solving math word problems with process-and outcome-based feedback. *arXiv preprint arXiv:2211.14275*, 2022.

Ziyu Wan, Xidong Feng, Muning Wen, Stephen Marcus McAleer, Ying Wen, Weinan Zhang, and Jun Wang. Alphazero-like tree-search can guide large language model decoding and training. In *Forty-first International Conference on Machine Learning*, 2024.

Ke Wang, Junting Pan, Weikang Shi, Zimu Lu, Houxing Ren, Aojun Zhou, Mingjie Zhan, and Hongsheng Li. Measuring multimodal mathematical reasoning with math-vision dataset. *Advances in Neural Information Processing Systems*, 37:95095–95169, 2025.

Peiyi Wang, Lei Li, Zhihong Shao, RX Xu, Damai Dai, Yifei Li, Deli Chen, Y Wu, and Zhifang Sui. Math-shepherd: A label-free step-by-step verifier for llms in mathematical reasoning. *arXiv preprint arXiv:2312.08935*, 2023.

Jason Wei, Xuezhi Wang, Dale Schuurmans, Maarten Bosma, Fei Xia, Ed Chi, Quoc V Le, Denny Zhou, et al. Chain-of-thought prompting elicits reasoning in large language models. *Advances in neural information processing systems*, 35:24824–24837, 2022.

Huajian Xin, ZZ Ren, Junxiao Song, Zhihong Shao, Wanxia Zhao, Haocheng Wang, Bo Liu, Liyue Zhang, Xuan Lu, Qiushi Du, et al. Deepseek-prover-v1. 5: Harnessing proof assistant feedback for reinforcement learning and monte-carlo tree search. *arXiv preprint arXiv:2408.08152*, 2024.

Guowei Xu, Peng Jin, Li Hao, Yibing Song, Lichao Sun, and Li Yuan. Llava-o1: Let vision language models reason step-by-step. *arXiv preprint arXiv:2411.10440*, 2024.

Huanjin Yao, Jiaxing Huang, Wenhao Wu, Jingyi Zhang, Yibo Wang, Shunyu Liu, Yingjie Wang, Yuxin Song, Haocheng Feng, Li Shen, et al. Mulberry: Empowering mllm with o1-like reasoning and reflection via collective monte carlo tree search. *arXiv preprint arXiv:2412.18319*, 2024.

Shunyu Yao, Dian Yu, Jeffrey Zhao, Izhak Shafran, Tom Griffiths, Yuan Cao, and Karthik Narasimhan. Tree of thoughts: Deliberate problem solving with large language models. *Advances in neural information processing systems*, 36:11809–11822, 2023.

Yixin Ye, Zhen Huang, Yang Xiao, Ethan Chern, Shijie Xia, and Pengfei Liu. Limo: Less is more for reasoning. *arXiv preprint arXiv:2502.03387*, 2025.

Renrui Zhang, Dongzhi Jiang, Yichi Zhang, Haokun Lin, Ziyu Guo, Pengshuo Qiu, Aojun Zhou, Pan Lu, Kai-Wei Chang, Yu Qiao, et al. Mathverse: Does your multi-modal llm truly see the diagrams in visual math problems? In *European Conference on Computer Vision*, pp. 169–186. Springer, 2024a.

Ruohong Zhang, Bowen Zhang, Yanghao Li, Haotian Zhang, Zhiqing Sun, Zhe Gan, Yinfai Yang, Ruoming Pang, and Yiming Yang. Improve vision language model chain-of-thought reasoning. *arXiv preprint arXiv:2410.16198*, 2024b.

Xiaoman Zhang, Chaoyi Wu, Ziheng Zhao, Weixiong Lin, Ya Zhang, Yanfeng Wang, and Weidi Xie. Pmc-vqa: Visual instruction tuning for medical visual question answering. *arXiv preprint arXiv:2305.10415*, 2023.

Fei Zhao, Taotian Pang, Chunhui Li, Zhen Wu, Junjie Guo, Shangyu Xing, and Xinyu Dai. Alignngpt: Multi-modal large language models with adaptive alignment capability. *arXiv preprint arXiv:2405.14129*, 2024.

Yilun Zhao, Yunxiang Li, Chenying Li, and Rui Zhang. Multihiertt: Numerical reasoning over multi hierarchical tabular and textual data. *arXiv preprint arXiv:2206.01347*, 2022.

Yaowei Zheng, Richong Zhang, Junhao Zhang, Yanhan Ye, Zheyuan Luo, Zhangchi Feng, and Yongqiang Ma. Llamafactory: Unified efficient fine-tuning of 100+ language models. In *Proceedings of the 62nd Annual Meeting of the Association for Computational Linguistics (Volume 3: System Demonstrations)*, Bangkok, Thailand, 2024. Association for Computational Linguistics. URL <http://arxiv.org/abs/2403.13372>.

Yaowei Zheng, Junting Lu, Shenzhi Wang, Zhangchi Feng, Dongdong Kuang, and Yuwen Xiong. Easyr1: An efficient, scalable, multi-modality rl training framework. <https://github.com/hiyouga/EasyR1>, 2025.

Deyao Zhu, Jun Chen, Xiaoqian Shen, Xiang Li, and Mohamed Elhoseiny. Minigpt-4: Enhancing vision-language understanding with advanced large language models. *arXiv preprint arXiv:2304.10592*, 2023.

Wenwen Zhuang, Xin Huang, Xiantao Zhang, and Jin Zeng. Math-puma: Progressive upward multimodal alignment to enhance mathematical reasoning. *arXiv preprint arXiv:2408.08640*, 2024.

A EXPERIMENT SETTINGS

Dataset and Benchmarks. To obtain the cold-start dataset, we use the multimodal visual question answering (VQA) datasets, LLaVA-CoT dataset (100K) (Xu et al., 2024) and Mulberry dataset (260K) (Yao et al., 2024), to conduct Vision-R1-cold (200K). During GRPO process, we mix the math datasets of We-Math (Qiao et al., 2024), MathVision (Wang et al., 2025), Polymath (Gupta et al., 2024), SceMQA (Liang et al., 2024), Geometry3K (Lu et al., 2021a) as our RL training data. Total amount of data is around 10K. For scaling up the RL dataset for Vision-R1-32B and Vision-R1-72B, we render text-based AIME data before 2024 as images, extract a subset from MAmmoTH-VL (Guo et al., 2024) and MMIQ (Cai et al., 2025), obtaining a total of $\sim 20K$ additional data.

For evaluating the reasoning capability of our Vision-R1, we choose three widely used multimodal math benchmarks: MM-Math (Sun et al., 2024), MathVista (Lu et al., 2023a), MathVerse (Zhang et al., 2024a). These benchmarks covers various mathematical fields which can provide a thorough evaluation of MLLMs’ math reasoning ability. Besides, we select four general multimodal benchmarks to demonstrate the general ability of our model: MMStar (Chen et al., 2024b), ChartQA (Masry et al., 2022), MME (Fu et al., 2023) and HallBench (Guan et al., 2024). Those general benchmarks are used to evaluate the data quality of our proposed Vision-R1-cold dataset.

Implementation Details. For the Vision-R1-cold dataset preparation, we deploy the open-source MLLM Qwen2.5-VL-72B (Bai et al., 2025) and the reasoning LLM DeepSeek-R1 (DeepSeek-AI, 2025). We then process the VQA datasets using Qwen-2.5-VL-72B and DeepSeek-R1.

For the cold-start initialization of Vision-R1, we adopt Qwen2.5-VL (Bai et al., 2025) as the base model and train it via supervised fine-tuning (SFT) for 2 epochs using Llama-Factory framework (Zheng et al., 2024). After cold-start initialization, we obtain the post-cold-start model, Vision-R1-CI, which is subsequently trained on the collected math dataset using GRPO in Verl training framework (Sheng et al., 2024; Zheng et al., 2025), while following the two-stage PTST approach (note that we do not use the third stage checkpoints), *i.e.*, S was set to 2. The all models in the paper are summarised as follows:

- **Vision-R1-Zero:** This represents the baseline approach where reinforcement learning (RL) is applied directly to the base MLLM without cold-start initialization. We adopt the limit of 4K generation token length with 16 samples to train the base model via RL training. The system prompt and the training method are described in Sec. 3.1. The full training step is set to 300.
- **Vision-R1-CI:** The base MLLM is cold-start initialized using the Vision-R1-cold dataset, resulting in this model.
- **Vision-R1-Long:** This variant is trained with a maximum generation length of 16K tokens, where four samples per input are generated from the cold-started Vision-R1-CI, followed by 300 training steps.
- **Vision-R1:** This model follows the Progressive Thinking Suppression Training (PTST) strategy, where a two-stage RL training process is applied:
 - **Stage 1:** The model is trained from Vision-R1-CI for 100 steps with an 4K token generation limit, sampling 16 samples per input.
 - **Stage 2:** Training continues for another 100 steps with a maximum generation length of 8K tokens, sampling 8 samples per input.

The final model checkpoint at the end of Stage 2 is the final Vision-R1 model, as this stage achieves an optimal balance between reasoning length and overall performance. Note that for **Vision-R1-32B** and **Vision-R1-72B**, we use additional data to continue training them in the RL stage under the same PTST Stage 2 settings.

Additionally, Vision-R1 can be further extended to a third training stage, following the same parameter settings as Vision-R1-Long and continuing for an additional 100 training steps. However, as shown in Fig. 1, further training does not yield significant performance improvements but does generate more complex reasoning processes.

For the ablation study experiments in Sec 4.2, we choose Vision-R1-7B as the default to evaluate. In Tab. 5 and Tab. 6, we chose the optimal checkpoint for reporting performance by evaluating every

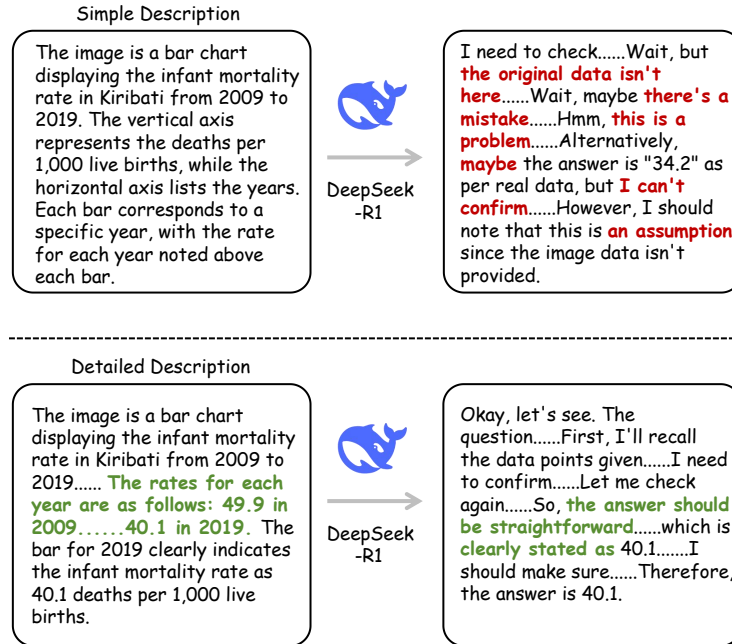


Figure 5: Comparison between the CoT processes generated by descriptions with and without “Pseudo-CoT”. Simple descriptions generated without the “Pseudo-CoT” input lack sufficient visual information, leading to confusion and hallucination in the reasoning process of DeepSeek-R1. In contrast, detailed descriptions enhanced through our Modality Bridging with “Pseudo-CoT” integrate high-quality visual information into textual descriptions, which facilitates accurate reasoning and enables R1 to generate correct answers.

fifth step in the final 50 steps of the RL training process, thereby avoiding the statistical bias caused by training instability.

To assess the quality of the Vision-R1-cold dataset, we apply the same training hyper-parameters of the cold-start initialization to Llama-3.2-V-Instruct (Dubey et al., 2024) for SFT, resulting in another post-cold-start MLLM, **Vision-R1-LlamaV-Cl**, which can also be used for subsequent RL training.

B COT COMPARISON FOR DATA CONSTRUCTION STRATEGY

We compare the CoT example generated by descriptions with and without “Pseudo-Co” in Fig. 5. When we directly use the naive image description as the input for DeepSeek-R1, the strong reasoning LLM cannot generate the correct trajectories for a massive amount of VQA data. This is because the MLLM does not know which image information is important for reasoning, and the generated image description lacks key converted image information, resulting in unusual CoT data.

C ADDITIONAL DATASET ILLUSTRATIONS

We provide some more examples of our Vision-R1-cold dataset in Fig. 6. Fig. 7 showcases multiple response instances generated by our Vision-R1 model, including comprehensive reasoning processes and corresponding final answers.

D DATA SOURCES

Our proposed Vision-R1-cold dataset consists of a wide range of multimodal data, including the following categories:

- Mathematical Data: GLLaVA (Gao et al., 2023), GEOS (Seo et al., 2015), UniGeo (Chen et al., 2022), GeoQA Plus (Chen et al., 2021), Geo3K (Lu et al., 2021a), MathVision (Wang

Question: Given a cone with a base radius represented by the variable 'r' ($r = 1$) and a slant height represented by the variable 's' ($s = 3$), determine the lateral surface area using variables.
 Choices: A: 2π B: 3π C: 6π D: 8π

<think> Okay, let's see. The problem is asking for the lateral surface area of a cone using the given variables r and s . The image shows illustrates that the formula is $L = \pi * r * s$. The radius r is 1, and the slant height s is 3. Plugging those values in, we multiply $\pi * 1 * 3$, which gives 3π . Looking at the choices, option B is 3π . That matches the calculation. So the answer should be B. </think> Final Answer: B </answer>

Question: The diamond ABCD is characterized by the side length AB as 'm' units ($m = 5$) and the side length AC as 'n' units ($n = 8$). Determine the area of the diamond using the given side lengths and locate the point of intersection O of the diagonals within the diamond.
 Choices: A: 40 B: 20 C: 48 D: 24

<think> Okay, so I need to find the area of this diamond-shaped quadrilateral ABCD. From the image, it's a rhombus because the diagonals bisect each other at right angles, forming four congruent right triangles. The formula given is $\text{Area} = 1/2 * d1 * d2$, where $d1$ and $d2$ are the lengths of the diagonals. They mention that $AC = 8$ units, so that's one diagonal ($d1 = 8$). The problem is that the other diagonal, BD , isn't given directly. However, we know the side length AB is 5 units. Since the diagonals of a rhombus bisect each other at right angles, each half of the diagonals forms legs of a right triangle, with the side of the rhombus as the hypotenuse. Let me visualize this. The diagonals intersect at point O, which is the midpoint of both diagonals. So $AO = AC/2 = 8/2 = 4$ units. Let's call BO the other half-diagonal, which would be $BD/2$. Since triangle AOB is a right triangle with legs $AO = 4$ and $BO = (BD/2)$, and hypotenuse $AB = 5$, Using the Pythagorean theorem here: $AO^2 + BO^2 = AB^2$. Plugging the numbers: $4^2 + BO^2 = 5^2 \rightarrow 16 + BO^2 = 25 \rightarrow BO^2 = 9 \rightarrow BO = 3$. Therefore, $BD = 2 * BO = 6$ units. Now, using the area formula: $1/2 * AC * BD = 1/2 * 8 * 6 = 24$. Wait, but 8^2 is 64, half of that is 24. But looking at the choices, D is 24. But wait, maybe I made a mistake. Let me double-check. Yes, AC is 8, BD is 6. So area is $(8*6)/2 = 24$. So D is correct. But wait, the problem shows "diamond ABCD is characterized by the side length AB as 'm' units ($m = 5$) and the side length AC as 'n' units ($n = 8$)". Wait, maybe I misunderstood. AC is a diagonal, not a side. So the given side length AB is 5, and diagonal AC is 8. So my calculation is correct. So the area is 24, choice D. </think> Final Answer: D </answer>

Question: Find JL .
 Choices: A: 3 B: 6 C: 12 D: 24

<think> Okay, let's see. So there's a triangle JKL with a perpendicular bisector MK . MK divides the triangle into two congruent triangles, right? And JM is 6. They want the length of JL . First, since MK is a perpendicular bisector, that should mean that M is the midpoint of JL . Because a bisector splits a line into two equal parts. So if MK is the perpendicular bisector of JL , then JM must equal ML . Since JM is 6, ML should also be 6. Therefore, $JL = JM + ML = 6 + 6 = 12$ units. Looking at the choices, C is 12. So the answer should be C. Let me double-check. The problem shows MK is a perpendicular bisector, so yes, M is the midpoint. The congruent segments JM and ML are both 6, so JL is 12. Yep, that makes sense. No other options fit. </think> Final Answer: C </answer>

Question: Is there luggage?


<think> Okay, let's see. The question is asking if there's luggage in the image depicted. The image depicts shows that some people are carrying or handling luggage, and there are visible suitcases and travel bags. That clearly indicates the presence of luggage. The scene is at a train platform with passengers waiting to board, which makes sense they would have luggage. So the answer should be yes. </think> Final Answer: yes </answer>

Figure 6: Examples of our Vision-R1-cold data. It comprises abundant information obtained through our Modality Bridging method.

Question: As shown in the figure, it is known that angle 1 = angle 2 = angle 3 = 55.0, then the degree of angle 4 is ()
 Choices: A:110' B:115' C:120' D:125'

<think> Okay, let's see. The problem displays that angles 1, 2, and 3 are each 55 degrees. Angle 4 is adjacent to angle 3 and they form a linear pair. A linear pair adds up to 180 degrees. So, if angle 3 is 55 degrees, then angle 4 must be 180 minus 55. Let me calculate that: $180 - 55$ is 125. So angle 4 should be 125 degrees. Looking at the choices, D is 125'. That must be the answer. </think> Final Answer: D </answer>

Question: As shown in the figure, $AC = BC$, AD bisects angle CAB , then the perimeter of triangle DBE is ()
 Choices: A:6cm B:7cm C:8cm D:9cm

<think> Okay, let's see. The problem displays that AC equals BC , so triangle ABC is isosceles with $AC = BC$. That means angles at A and B are equal. AD bisects angle CAB , so angle CAD is equal to angle DAB . Since ABC is isosceles, the angle at A is split into two equal parts by AD . Now, there's a line DE perpendicular to AC , meeting at E . The perimeter of triangle DBE is what we need to find. The answer choices are 6, 7, 8, or 9 cm. The image mentioned that the perimeter is equal to AB , which is 6 cm. Wait, but AB is 6 cm. So if the perimeter of triangle DBE is equal to AB , then the answer should be 6 cm, which is option A. But let me make sure I didn't miss anything. The problem displays that $AC = BC$, and AD is an angle bisector. DE is perpendicular to AC . Maybe there's a property here where the perimeter of DBE equals AB because of some triangle congruence or something. Since the image displays displays the perimeter is equal to AB , which is 6 cm, then the answer is A. </think> Final Answer: A </answer>

Question: As shown in the figure, PA and PB are tangent to circle O at A and B respectively. If angle $C = 65.0$, then the degree of angle P is ()
 Choices: A:65' B:130' C:50' D:100'

<think> Okay, let's see. The problem is about tangents to a circle from an external point. PA and PB are tangents touching the circle at A and B. The angle at C is 65 degrees, and we need to find the measure of angle P. First, I remember that the two tangent segments from a single external point to a circle are equal in length. So PA equals PB . That makes triangle PAB an isosceles triangle with $PA = PB$. But the question is about angle P, which is the angle between the two tangents. There's a property in geometry that displays the angle between two tangents from an external point is equal to 180 degrees minus the measure of the central angle subtended by the points of contact. Alternatively, another way to think about it is that the angle between the tangents (angle P) is supplementary to the measure of the central angle AOB . So if I can find the measure of angle AOB , then angle P would be $180^\circ - \text{angle } AOB$. But how do I find angle AOB ? Well, the points A and B are points of contact on the circle. The angle at the center, angle AOB , is related to the arc AB. The measure of angle AOB is equal to the measure of the arc AB in degrees. On the other hand, the angle at point C is given as 65 degrees. Since point C is in the circle, angle ACB is an inscribed angle. The measure of an inscribed angle is half the measure of its intercepted arc. So angle ACB intercepts arc AB , which means arc AB is $2 * 65^\circ = 130^\circ$. Therefore, the central angle AOB is 130 degrees. Then, angle P is $180^\circ - 130^\circ = 50^\circ$. Let me double-check. If angle AOB is 130°, then the angle between the tangents (angle P) is $180^\circ - 130^\circ = 50^\circ$. That makes sense. The answer is C. </think> Final Answer: C </answer>

Question: As shown in the figure, the plant spacing (the horizontal distance between two adjacent trees) is required to be 4.0. If trees are planted on a hillside with a slope of 0.75, and the plant spacing is also required to be 4.0, then the slope distance between two adjacent trees is ()
 Choices: A:5m B:6m C:7m D:8m

<think> Okay, let's see. The problem is about finding the slope distance between two adjacent trees on a hillside. The horizontal distance between them is 4.0 meters, and the slope of the hillside is 0.75. Hmm, slope is usually rise over run. So if the slope is 0.75, that means for every 1 meter horizontal distance, the vertical change is 0.75 meters. But here, the horizontal distance between the trees is 4.0 meters. So I need to find the vertical change over that 4 meters. Wait, the slope is 0.75, so the vertical change (let's call it v) for a horizontal run (r) of 4 meters would be $v = 0.75 * r$. So $v = 0.75 * 4 = 3$ meters. So the vertical difference is 3 meters. Now, the slope distance would be the hypotenuse of a right triangle with horizontal leg 4 meters and vertical leg 3 meters. Using the Pythagorean theorem, the slope distance (d) is $\sqrt{4^2 + 3^2} = \sqrt{16 + 9} = \sqrt{25} = 5$ meters. So the answer should be A:5m. </think> Final Answer: A </answer>

Figure 7: More output examples of our Vision-R1-7B on MathVerse benchmark.

et al., 2025), GeoMverse (Kazemi et al., 2023), MathV360K (Shi et al., 2024), IconQA (Lu et al., 2021b), TabMWP (Lu et al., 2023b), CLEVR (Johnson et al., 2017), CLEVR-Math (Lindström & Abraham, 2022), and Super-CLEVR (Li et al., 2023).

- General QA Data: ShareGPT4V (Chen et al., 2024a), PISC (Li et al., 2017) VQA-AS (Antol et al., 2015), A-OKVQA (Schwenk et al., 2022), TextVQA (Singh et al., 2019), Vizwiz (Gurari et al., 2018), and VQA2.0 (Goyal et al., 2017)

- Science and Medical Data: From GeoQA+ (Cao & Xiao, 2022), CLEVR-Math (Lindström & Abraham, 2022), TQA (Kembhavi et al., 2017), AI2D (Kembhavi et al., 2016), ScienceQA (Lu et al., 2022), VQA-RAD (Lau et al., 2018), and PMC-VQA (Zhang et al., 2023)
- Figure Understanding Data: From DVQA (Kafle et al., 2018), DocVQA (Mathew et al., 2021), FigureQA (Kahou et al., 2017), PlotQA (Methani et al., 2020), ChartQA (Masry et al., 2022), InfoVQA (Mathew et al., 2022), MultiHierTT (Zhao et al., 2022), and LRV-Chart (Liu et al., 2023).

E LLM USAGE

In this paper, we have used an LLM to refine some sentences and improve the grammar, making the paper more academic.